

One-Dimensional Constrained Blister Test to Measure Thin Film Adhesion

Tingting Zhu

Mechanical and Industrial Engineering,
Northeastern University,
Boston, MA 02115

Sinan Müftü

Mechanical and Industrial Engineering,
Northeastern University,
Boston, MA 02115

Kai-tak Wan¹

Mechanical and Industrial Engineering,
Northeastern University,
Boston, MA 02115
e-mail: ktwan@coe.neu.edu

A rectangular film is clamped at the opposite ends before being inflated into a blister by an external pressure, p . The bulging film adheres to a constraining plate with distance, w_0 , above. Increasing pressure expands the contact area of length, $2c$. Depressurization shrinks the contact area and ultimate detaches the film. The relation of (p, w_0, c) is established for a fixed interfacial adhesion energy. [DOI: 10.1115/1.4039171]

Keywords: thin film, adhesion, delamination, constrained blister, pull-off

Thin film adhesion is crucial in determining the reliability and lifespan of nano-/micro-electronics parts and devices. We recently revisited the classical constrained blister test where a freestanding circular membrane clamped at the edge is pressurized to make adhesion contact with a constraining plate [1]. The relation between the measurable quantities of deformed film geometry, applied pressure, and contact radius, the materials parameters of interfacial adhesion energy and elastic modulus, and the spontaneous pull-off at critical pressure, are established based on a thermodynamic energy balance. In this paper, we extend the theoretical model to a rectangular film, and briefly compare the behavior of one-dimensional (1D) to two-dimensional (2D) geometry. Interested readers should refer to the earlier paper for engineering applications.

Figure 1 shows a linear elastic, rectangular film with unit width, length, $2a$, thickness, h , elastic modulus, E , Poisson's ratio, ν , and negligible flexible rigidity is clamped at its two opposite edges. External pressure, p , pushes the film into adhesion contact with a planar constraining plate a distance, w_0 , above, and a force per unit width, F , is necessary to hold the plate in equilibrium. The deformed film profile, $w(x)$, has a contact length, $2c$, and angle, θ , at the contact edge. Within the contact area, $w(x \leq c) = w_0$. In the freestanding sections ($c < |x| \leq a$), the film inclines at an angle $\psi \approx \partial w / \partial x$ and $\psi(x = c) = \theta$. For simplicity, all physical quantities (bold) are made dimensionless (plain) based on

$$\begin{aligned} w &= \frac{w}{h}, \quad w_0 = \frac{w_0}{h}, \quad c = \frac{c}{a}, \quad x = \frac{x}{a} \\ \gamma &= \gamma \left[\frac{6(1-\nu^2) a^4}{Eh^5} \right], \quad F = F \left[\frac{3(1-\nu^2) a^3}{Eh^4} \right], \\ p &= p \left[\frac{6(1-\nu^2) a^4}{Eh^4} \right], \quad G = G \left[\frac{6(1-\nu^2) a^4}{Eh^5} \right], \\ \sigma &= \sigma \left[\frac{12(1-\nu^2) a^2}{Eh^2} \right], \quad \psi = \frac{dw}{dx} = \left(\frac{a}{h} \right) \frac{dw}{dx} = \frac{a}{h} \times \psi \end{aligned}$$

Balance of vertical forces requires $2x \cdot p - F = 2\sigma h \cdot \sin \psi \approx 2\sigma h \cdot \psi$ for small ψ , or, equivalently, $\psi = (2p/\sigma) \cdot (x - 1/\Phi)$ with $\Phi = p/F$ and $\Phi(\theta = 0) = 1/c$. Integration yields

$$w(x) = \int_x^1 \psi \cdot dr = w_0 \times \left[\frac{2(1-x) - (1-x^2)\Phi}{2(1-c) - (1-c^2)\Phi} \right] \quad (1)$$

The elastic strain, ϵ , is uniform in the overhanging sections ($c < |x| \leq 1$). Simple energy consideration yields the mechanical response given by

$$p = 8w_0^3 \times \left\{ \frac{(1+c+c^2)\Phi^3 - 3(1+c)\Phi^2 + 3\Phi}{(1-c)^3 [(c+1)\Phi - 2]^3} \right\} \quad (2)$$

Equation (2) is valid during the loading stage when pressure increases. Thermodynamic energy balance yields the strain energy release rate given by [2]

$$G = \sigma \cdot h \left(\frac{\theta^2}{2} \right) + \frac{E \cdot h}{2(1-\nu^2)} (\epsilon - \epsilon_0)^2 \quad (3)$$

with ϵ and ϵ_0 the membrane strain in the freestanding section and contact area, respectively. No delamination is expected for $G < \gamma$. As p exceeds a critical threshold, G reaches the adhesion energy with $G = \gamma$, and the film delaminates from the plate. Substituting Eq. (2) into Eq. (3)

$$\gamma = f_1 \cdot p^{4/3} + 3(f_2 \cdot p^{2/3} - \epsilon_0)^2 \quad (4)$$

where the functions are defined as

$$\begin{aligned} f_1(c, \Phi) &= \frac{(c\Phi - 1)^2}{2 \{ (1+c+c^2)\Phi^6 - 3(1+c)\Phi^5 + 3\Phi^4 \}^{1/3}} \\ f_2(c, \Phi) &= \frac{\{ (1+c+c^2)\Phi^2 - 3(1+c)\Phi + 3 \}^{1/3}}{6\Phi^{2/3}} \end{aligned}$$

To illustrate the model, Fig. 2 shows the special cases of $\gamma = 5$ and $\gamma = 20$ for a gap of $w_0 = 1$. Figure 3 shows the corresponding deformed profile. Along path OA, initial pressurization causes the film to bulge but yet to make contact with the plate ($c = 0$ and $\Phi \rightarrow \infty$) and $p = 8w_0^3$ from Eq. (2), where the blister height $w_0(p)$ is a monotonic increasing function. At A, $p = 8$ and the film touches the plate with a line contact. Increase in p along AB expands the contact area and raises F with $F = p \cdot c$, though θ

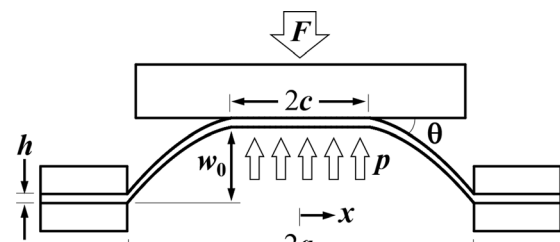


Fig. 1 Schematic of a pressurized 1D rectangular film adhering to a rigid constraining plate above

¹Corresponding author.

Manuscript received December 18, 2017; final manuscript received January 29, 2018; published online March 2, 2018. Editor: Yonggang Huang.

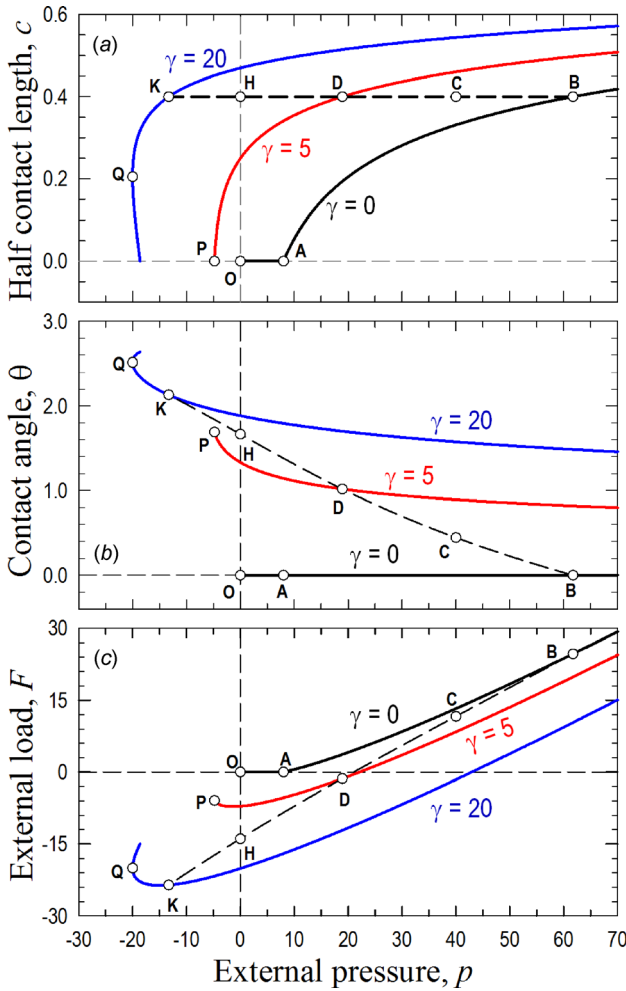


Fig. 2 Mechanical response of (a) contact length, c , (b) contact angle, θ , and (c) force to keep plate in equilibrium, F , as functions of applied pressure for $w_0 = 1$ and fixed adhesion energy. Initial loading along OA causes the film to bulge but yet to touch the plate. For $\gamma = 5$, pressurization along AB causes (a) contact to expand from null to maximum, (b) θ to remain at zero, and (c) F to increase to counterbalance the rising pressure. Initial depressurization along BCD causes (a) c to remain constant, (b) θ to increase to raise G , and (c) F to diminish. Further decrease in p causes delamination along DP, where (a) contact shrinks, (b) θ to rise further, and (c) F to diminish further. Pinch-off occurs at P when the contact area reduces to a line and the film spontaneously detaches from the plate. Stronger adhesion with $\gamma = 20$ retraces the loading path OAB. Initial depressurization along BCDHK where the contact remains unchanged. Further decrease in p leads to delamination along KQ. Pull-off occurs at Q when $dp/dc = 0$.

remains at 0. The residual stress locked up in the contact area, $\sigma_0(x)$, increases from the center to a maximum with $\sigma_0(x=c) = \sigma$, and is continuous into the freestanding sections. Depressurization at B does not lead to immediate delamination, since $\theta = 0$ implying $G = 0 < \gamma$. Along BCD, θ increases and raises G until the onset of delamination where $G = \gamma$ at D. Further decrease in p along DP shrinks the contact area according to Eq. (4). The mechanical response during delamination, $p(c, w_0)$, for a fixed γ can therefore be determined in a self-consistent manner. At P, the film turns into a cusp making a line contact with the plate. Incremental increase in suction leads to spontaneous pinch-off where $c^* = 0$ at the critical pressure p^* . In a strong membrane–plate interface with $\gamma = 20$, depressurization proceeds along BCDHK raising G from zero to $G = \gamma$. Delamination occurs along KQ. At Q, $p^* \approx -\gamma/w_0$ and $dp/dc = 0$, further decrease in p can no longer follow the

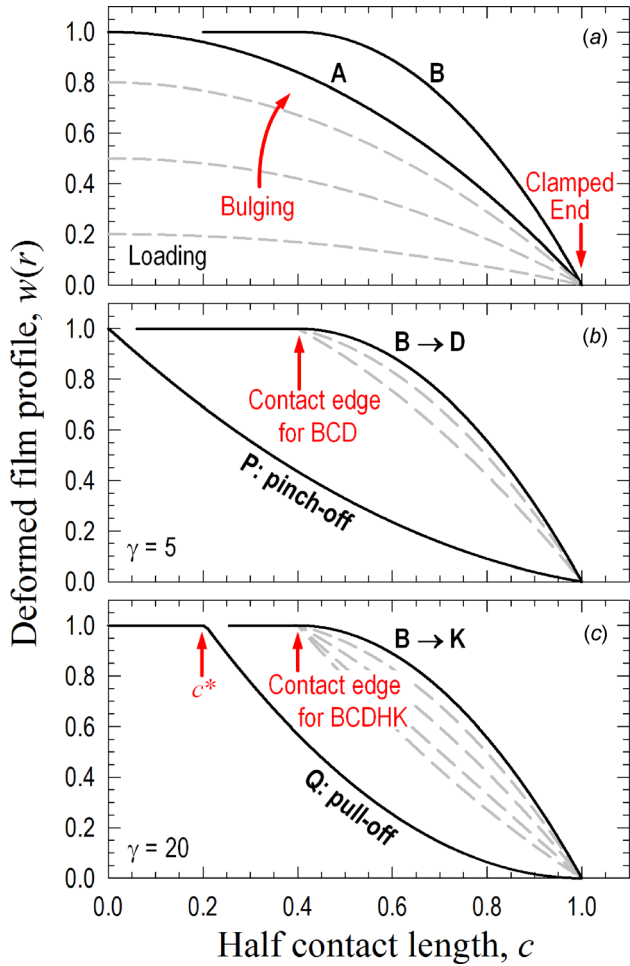


Fig. 3 Changing film profile for $w_0 = 1$. (a) Initial pressurization along OAB causes the film to bulge and the contact to expand. (b) For $\gamma = 5$, pressure decreases along BCDP. Along BCD, the contact area remains unchanged but θ increases. Delamination occurs along DP until pinch-off at P . (c) For $\gamma = 20$, pressure decreases along BCDHKQ with pull-off at Q . The curves are labeled based on Fig. 2.

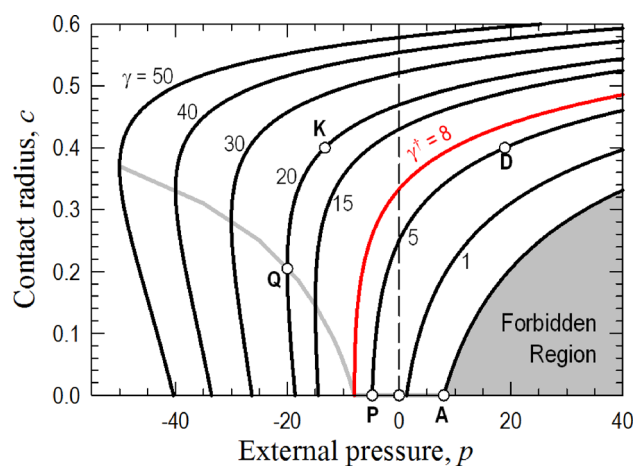


Fig. 4 Contact length as a function of applied pressure for $w_0 = 1$ and a range of adhesion energy. The lowest curve corresponds to $\gamma = 0$, and the area underneath is forbidden. Curves labeled $\gamma = 5$ and $\gamma = 20$ correspond to those shown in Figs. 2 and 3. Curve labeled $\gamma^* = 8$ indicates the transition from pinch-off to pull-off. The locus of pull-off ($dp/dc = 0$) is shown as gray curve.

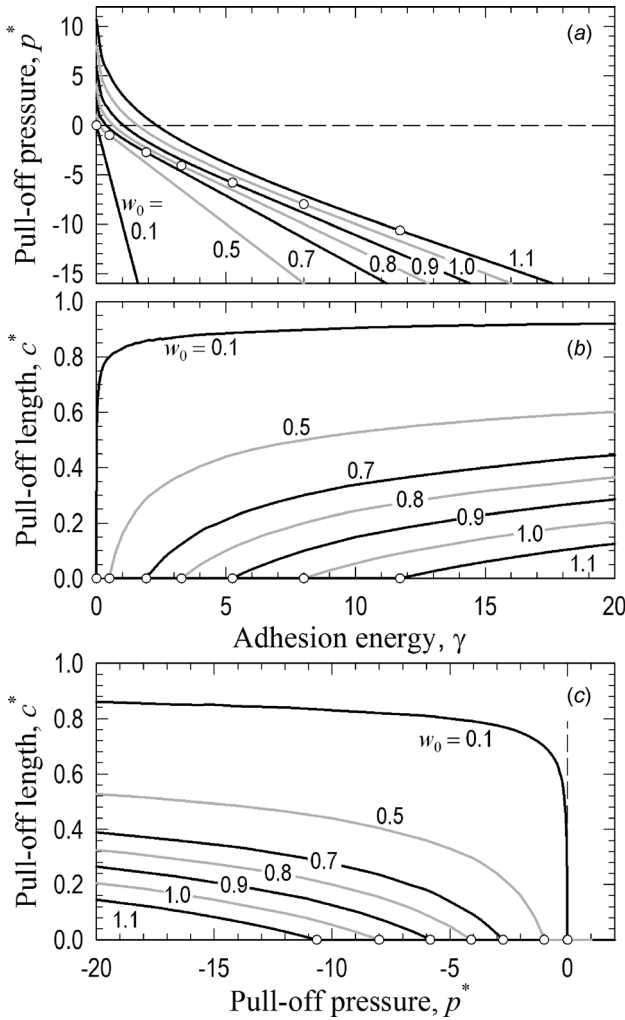


Fig. 5 Relations of “pull-off” parameters for a range of w_0 . (a) Critical pressure and (b) contact length as functions of adhesion energy with a range of gap w_0 . (c) Critical contact length as a function of critical pressure. The symbols denote the transition $\gamma = \gamma^*$ from pinch-off to pull-off.

energy balance and *pull-off* occurs with $c^* > 0$. Figure 4 shows a family of delamination curves for a range of γ with $w_0 = 1$, and the gray curve shows the pull-off locus, $c^*(p^*)$. Weak interface with $\gamma < \gamma^* = 8$ leads to pinch-off with $c^* = 0$. If w_0 is allowed to span a range, Eq. (4) yields

$$\gamma = 8w_0^4 \times \left\{ \frac{7\Phi^{*2} - 20\Phi^* + 19}{6(\Phi^* - 2)^4} \right\} \quad (5)$$

with $\Phi^* = p^*/F^* \leq 1$. The threshold governing the transition from pinch-off to pull-off is given by $\gamma^* = 8w_0^4$ with $\Phi^* = 1$ and $c^* = 0$

in Eq. (5). It is therefore possible experimentally to choose a specific w_0 to ensure pinch-off rather than pull-off. One interesting outcome from the present model is that if $\gamma_0 = 19w_0^4/12$, pinch-off occurs at $p^* = 0$ corresponding to a tensile force on the constraining plate of $F^* = -3w_0^3$, which is consistent with our earlier work in a 1D punch test in the absence of pressure [3].

Figure 5 shows the interrelation of the pinch-off/pull-off parameters (c^* , p^* , w_0 , γ). It is worthwhile to compare the current 1D results with the two-dimensional (2D) circular film counterpart [1]. Figures 5(a) and 5(b) shows the monotonic decreasing $p^*(\gamma)$ and increasing $c^*(\gamma)$, respectively, which are similar to the 2D counterpart. Figure 5(c) shows that 1D pinch-off is possible as long as $\gamma < \gamma^*$, and pull-off always requires suction ($p^* < 0$). In contrary, 2D allows pinch-off only when $\gamma = 0$ and pull-off for $\gamma > 0$. Note also that $c^*(p^* = 0) = 0$ in 1D, but $c^*(p^* = 0) = 0.2060$ in 2D. The present model is useful in designing microelectromechanical devices as well as devising testing method to measure thin film adhesion.

As a last remark, it is noted that clamping only the two opposite edges of a rectangular film with finite width while applying a uniform pressure is practically challenging. One possible way to realize the configuration is to resort to a three-dimensional axisymmetric setup. A rectangular film wraps around the rims of two thick concentric circular plates of radius, R , separated by a small gap, $2a$, to create a hermetic setup to retain the applied pressure. A rectangular strip is then bent into a circle with diameter $2R + 2w_0$ to serve as the constraining plate. The present model has to be modified to accommodate the three-dimensional geometry and the new boundary conditions, but will nonetheless serve as a limiting case for $R \gg a$ and $R \rightarrow \infty$. Another possible geometry is to have a very wide rectangular film with a narrow freestanding portion, where our solution will be valid at the central region away from the edges.

Acknowledgment

Any opinions, findings, and conclusions or recommendations expressed in this material are those of the authors and do not necessarily reflect the views of the National Science Foundation.

Funding Data

- National Science Foundation (Grant No. CMMI # 1232046).

References

- [1] Zhu, T., Li, G., Muftu, S., and Wan, K.-T., 2017, “Revisiting the Constrained Blister Test to Measure Thin Film Adhesion,” *ASME J. Appl. Mech.*, **84**(7), p. 071005.
- [2] Williams, J. G., 1997, “Energy Release Rates for the Peeling of Flexible Membranes and the Analysis of Blister Tests,” *Int. J. Fract.*, **87**(3), pp. 265–288.
- [3] Li, G., and Wan, K. T., 2010, “Delamination Mechanics of a Clamped Rectangular Membrane in the Presence of Long-Range Intersurface Forces: Transition From JKR to DMT Limits,” *J. Adhes.*, **86**(3), pp. 335–351.